Proceedings of ASME Turbo Expo 2011
GT2011
June 6-10, 2011, Vancouver, British Columbia, Canada

GT2011-46184

EFFECTS OF THE SHAFT NORMAL MODES ON THE MODEL-BASED IDENTIFICATION OF UNBALANCES IN ROTATING MACHINES

A. Vania **P. Pennacchi** **S. Chatterton**
Politecnico di Milano, Dept. of Mechanical Engineering
Via La Masa, 1, I-20156, Milano, Italy

ABSTRACT

Model-based methods can be applied to identify the most likely faults that cause the experimental response of a rotating machine. Sometimes, the objective function, to be minimized in the fault identification method, shows multiple sufficiently low values that are associated with different sets of the equivalent excitations by means of which the fault can be modeled. In these cases, the knowledge of the contribution of each normal mode of interest to the vibration predicted at each measurement point can provide useful information to identify the actual fault. In this paper, the capabilities of an original diagnostic strategy that combines the use of common fault identification methods with innovative techniques based on a modal representation of the dynamic behavior of rotating machines is shown. This investigation approach has been successfully validated by means of the analysis of the abnormal vibrations of a large power unit.

INTRODUCTION

The increase of the performances of rotating machines and the reduction of the duration of the machine outages required to perform maintenance activities can be obtained by improving the capabilities of diagnostic techniques. With regard to this, fault identification methods, based on mathematical models of the rotor system, can give successful results.

In general, these diagnostic methods are based on the identification of a suitable set of excitations that allow obtaining a satisfactory simulation of the experimental dynamic behavior of the rotating machine. The identification of the best set of excitations can be performed by minimizing the error between the experimental vibration data and the respective theoretical vibrations predicted by the machine model. As the most important faults in rotating machines can be modeled by means of suitable sets of excitations having specific harmonic patterns, the identification of the best set of excitations that minimizes the objective function allows evaluating the severity, the location and the type of the faults to which a machine is subjected. The reliability of the results provided by the fault identification methods often depends on the accuracy of the machine model. Therefore, a preliminary model tuning is required. Anyway, in order to discard unreliable estimates of the faults, only the results that cause sufficiently low values of the objective function used in the identification process should be considered. However, sometimes, the identified faults that cause a rather small value of the objective function are more than one. This can cause some ambiguity in the determination of the actual fault. In this case it could be necessary to judge the reliability of the results provided by the fault identification methods by considering the indications of further uncommon diagnostic techniques.

In this paper, the contribution of the machine vibrations caused by the excitation of the single normal modes of the shaft-train to the global response of the rotor system has been studied by means of a new investigation method based on the use of the machine modal parameters. In fact, the knowledge of the more recent and the most important maintenance activities to which a machine has been subjected can be correlated to the energy introduced in the rotor system, by the identified excitations, for each normal mode of interest. In some occurrences, in which a satisfactory minimization of the objective function is given by more than one set of excitations, the results of this analysis can be decisive to identify the actual fault. This approach, based on modal analysis, differentiates this fault identification method from those of other authors.

In order to validate this diagnostic strategy, the abnormal dynamic behavior of the generator of a thermoelectric power unit has been analyzed. More than one likely fault has been identified by the model-based method. However, the analysis of the contribution of each normal mode to the system response gave significant information to discard unreliable solutions. Moreover, the same investigation procedure proved to be very useful to explain the reasons for the occurrence of the abnormal dynamic behavior of the rotating machine.

CASE STUDY

The machine-train of the power unit considered in this paper was composed of a high-pressure-intermediate-pressure (HP-IP) steam turbine, a low-pressure (LP) turbine and a generator. These machines were connected by means of rigid couplings. The machine-train diagram and the bearing numbers are shown in Figure 1, while a more detailed drawing of the generator rotor is shown in Figure 2. The rated power was 175 MW while the operating speed was 3000 rpm.

Each support was equipped with a pair of XY proximity probes, oriented 90 degrees apart, for measuring the shaft relative vibration. In addition to this, a pair of seismic transducers, mounted on the same measurement points of the proximity probes, measured the pedestal absolute vibration.

Some maintenance activities were performed on the generator during a long planned outage. This maintenance required to dismount the two rotor caps, located at the ends of the main body of the generator rotor, and to machine the flange of the coupling facing the LP turbine.

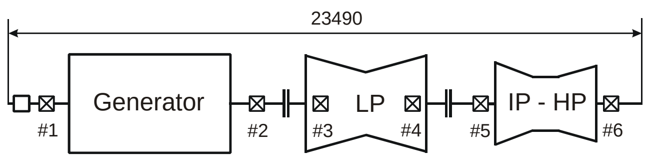

Figure 1. Machine-train and bearing numbers.

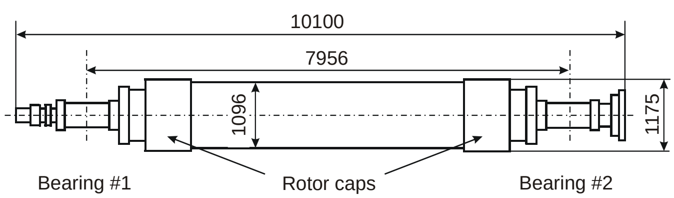

Figure 2. Drawing of the generator rotor.

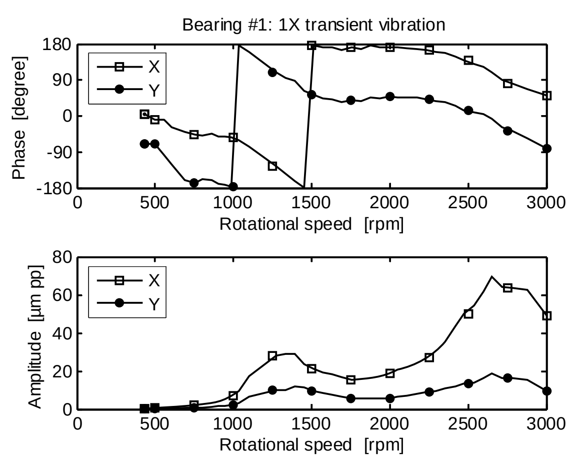

Figure 3. Bode plot of the 1X relative vibration measured at bearing #1, in the X and Y directions, during a runup performed before the maintenance.

The Bode plot of the synchronous (1 × rev., 1X) relative vibration of the generator measured at bearing #1, in the X and Y directions, during a runup performed few months before the maintenance, is shown in Figure 3. These experimental data point out that the first balance resonance of the shaft was close to 1300 rpm while the second flexural critical speed was close to 2600 rpm. When passing through these critical speeds and at the operating speed, the vibration levels were not very high: this indicates that before the maintenance the residual unbalance of the generator was not excessive.

The Bode plots of the 1X relative vibration of the generator measured at bearings #1 and #2, in the X and Y directions, during the first runup performed after the maintenance are shown in Figure 4 and Figure 5.

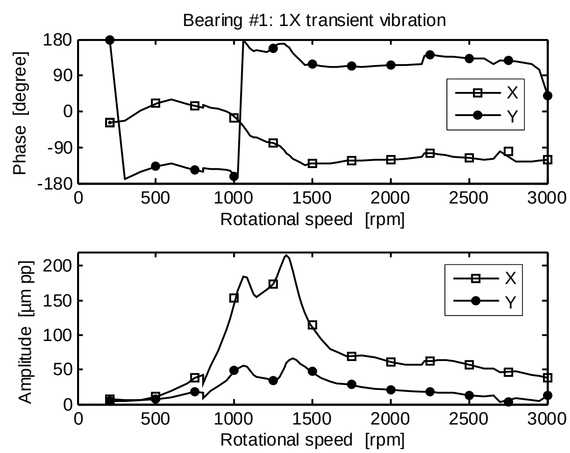

Figure 4. Bode plot of the 1X relative vibration measured at bearing #1 during the first runup performed after the maintenance.

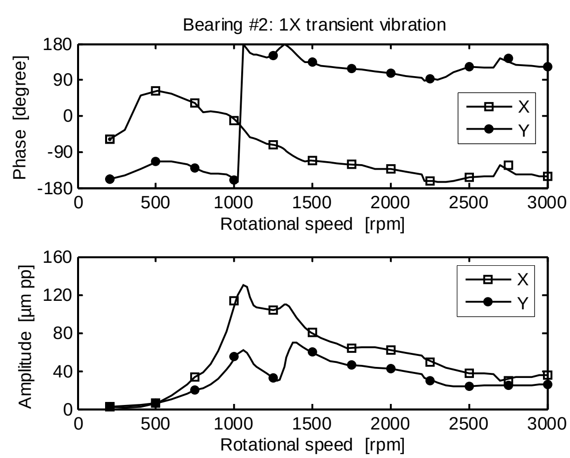

Figure 5. Bode plot of the 1X relative vibration measured at bearing #2 during the first runup performed after the maintenance.

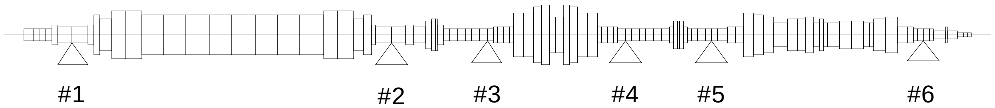

Figure 6. Finite element model of the shaft-train.

In the rotational speed range from 900 rpm to 1500 rpm the magnification of the level of these vibrations is considerable, especially at the outboard bearing #1. Owing to the anisotropy of the oil-film journal bearing the first balance resonance of the generator is spilt into two separated flexural critical speeds at 1060 rpm and 1330 rpm. At the latter rotational speed, on bearing #1, a maximum level of 221 μm pp was reached. Conversely, in the rotational speed range above 1750 rpm, the amplitude of the generator vibrations (1X) were lower than 70 μm pp. In particular, at the operating speed these levels were lower than 50 μm pp at each measurement point located on both bearings #1 and #2.

Moreover, when the rotational speed approached 2600 rpm, the vibration magnification caused by the passing through the flexural critical speed was negligible and also the phase of the 1X vibration vectors showed only minor changes. This behavior, which proved to be repetitive during further runups and coastdowns performed in the following days, is in contrast with that found before the maintenance.

MODEL-BASED ANALYSIS

In order to investigate the causes of this abnormal dynamic behavior of the generator, a mathematical model of the machine-train was developed. This model included the Finite Element Model (FEM) of the shaft-train illustrated in Figure 6, a model of each oil-film journal bearing and a model of the foundation structure [1, 2]. The FE model of the generator shaft only, is shown in detail in Figure 7 along with the numbers of some significant nodes of the FE mesh that will be cited in the description of investigations reported in the following. The axial coordinate of these significant nodes is reported in Table 1.

At first an eigenvalue analysis was carried out to verify the reliability of the predicted flexural critical speeds and shaft-train normal modes provided by the machine model.

The values of the first eight critical speeds of the shaft-train, obtained from a Campbell diagram, here not reported for the sake of brevity, are shown in Table 2 along with the dimensionless damping factors, h_r, a brief description of the shape of the corresponding normal mode and the indication of the machine that is mainly affected by each eigenmode. The critical speeds of the generator included in the rotational speed range below 3500 rpm correspond to the eigenvalues n.1, n.2 and n.7. The shape of the normal modes associated with these eigenvalues is shown in Figure 8.

The theoretical values of the first three flexural critical speeds of the generator are in good accordance with the respective experimental values. The shape of the first two normal modes is in accordance with a typical "U" bending mode of a shaft. The shape associated with the critical speed of 2538 rpm is a typical 2nd bending mode of a shaft having a "node" close to the middle of the span between the generator supports and out-of-phase displacements in the area close to the journal bearings #1 and #2 and to the caps.

Table 1. Axial coordinate of some significant nodes of the FEM of the generator rotor.

Node n.	Axial coordinate [mm]	Node n.	Axial coordinate [mm]
3	390	17	5179
7	1192	21	7435
9	1689	23	8181
11	2146	25	8638
13	2902	27	9148
16	4623	31	10092

Table 2. First eight flexural critical speeds of the shaft-train provided by the eigenvalue analysis.

N.	Critical Speed [rpm]	Damping Factor h_r	Machine	Bending Mode Order
1	1042	0.1174	Generator	1st
2	1372	0.0386	Generator	1st
3	1642	0.0406	LP Turbine	1st
4	1805	0.0370	HP-IP Turbine	1st
5	2130	0.0368	HP-IP Turbine	1st
6	2226	0.1155	LP Turbine	1st
7	2538	0.1544	Generator	2nd
8	3440	0.2042	LP Turbine	2nd

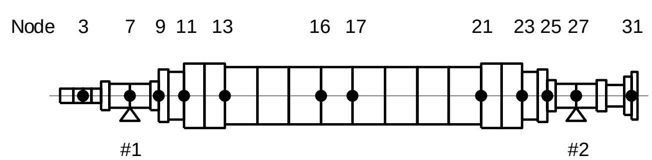

Figure 7. Finite element model of the generator rotor and identification number of some significant nodes.

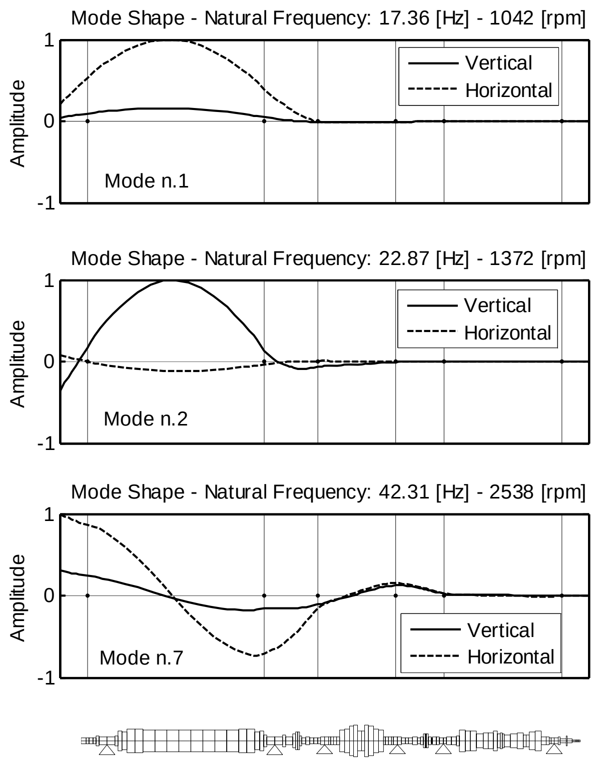

Figure 8. Shape of the shaft-train normal modes associated with the eigenvalues n.1, n.2 and n.7.

FAULT IDENTIFICATION METHOD

The experimental data collected after the maintenance, illustrated in Figures 4 and 5, show that at low rotational speeds the level of the 1X vibration of the generator was very low. Therefore, it was assumed that the runout, the shaft eccentricity and the dynamic effects caused by a possible machine misalignment were negligible.

Then, it was supposed that the considerable levels of the 1X vibration of the generator measured when passing through the first two critical speeds contained in the speed range from 900 rpm to 1500 rpm were caused by unbalances generated by an improper machine reassembling performed at the end of the maintenance. With regard to this, it is important to remark that no balancing activity was carried out before the unit restart.

It is well known that the most important faults in rotating machines can be modeled by means of suitable sets of equivalent excitations that can be applied to nodes of the FEM of the shaft-train [3-6]. In the past, the authors developed a model-based method aimed at identifying the best set of equivalent excitations that minimizes the error between the experimental vibrations of rotating machines and the respective numerical results provided by the simulation model [4].

In practice, a relative error, usually called residual, is often considered. The residual, ε, can be expressed as:

$$\varepsilon = \frac{\left(\boldsymbol{X}_{exp}^{*} - \boldsymbol{X}_{th}^{*}\right)^{T}\left(\boldsymbol{X}_{exp} - \boldsymbol{X}_{th}\right)}{\left(\boldsymbol{X}_{exp}^{*}\right)^{T}\left(\boldsymbol{X}_{exp}\right)} \tag{1}$$

where $\boldsymbol{X}_{exp}$ is a vector that contains the experimental vibrations collected at different measurement points and different rotational speeds, while the vector $\boldsymbol{X}_{th}$ contains the corresponding theoretical vibrations evaluated by means of the machine model in which the best set of equivalent excitation has been considered.

In order to obtain a normalized index, ranging from 0 to 1, that certifies the accuracy with which the identified faults are able to simulate the experimental vibrations, the Coherence Factor, γ, given by the following expression, can be used:

$$\gamma = \frac{\left|\left(\boldsymbol{X}_{exp}^{*}\right)^{T}\left(\boldsymbol{X}_{th}\right)\right|^{2}}{\left(\left(\boldsymbol{X}_{exp}^{*}\right)^{T}\left(\boldsymbol{X}_{exp}\right)\right)\left(\left(\boldsymbol{X}_{th}^{*}\right)^{T}\left(\boldsymbol{X}_{th}\right)\right)} \tag{2}$$

The fault identification method developed in the past by the authors can be applied to determine single faults or multiple faults [4]. As said above, each fault can be modeled by means of a suitable set of harmonic forces and moments whose magnitude, phase and axial position along the shaft-train is evaluated by the identification method. Therefore, this diagnostic strategy allows the severity, the location and the type of the fault to be identified. The most likely fault corresponds to the lowest value of the residual ε.

In this case study it was suspected that the abnormal 1X vibrations of the generator were caused by a significant residual unbalance.

Two unbalances hypothesis

Then, it was supposed that the dynamic effects caused by this fault could be modeled by means of two unbalances, denoted UA and UB, applied to different cross-sections of the generator rotor, whose axial position is defined by the node numbers, denoted “A” and “B”, of the shaft FE model.

The identification of the best pair of unbalances, that have been assumed to be applied to the generator rotor only, has been obtained considering the 1X experimental vibrations measured during a runup at nine significant rotational speeds contained between 900 rpm and 3000 rpm. The map of the residuals, ε, obtained by applying the fault identification method is shown in Figure 9. In this figure the axial position of the nodes “A” and “B” to which the unbalances UA and UB are applied is reported in the axes x and y, respectively. It is possible to note that the value of the residuals associated with some pairs of unbalances is rather low. This indicates that, among the large number of combinations of pairs of unbalances, some solutions that allow obtaining a good accordance between the generator experimental vibrations and numerical results exist.

Table 3. Optimal estimates of pairs of unbalances placed on different cross-sections of the generator to simulate the 1X experimental vibrations measured in the rotational speed range from 900 rpm to 3000 rpm.

	UNBALANCE UA			UNBALANCE UB				
Case	Node A n.	Magnitude [kgm]	Phase [degree]	Node B n.	Magnitude [kgm]	Phase [degree]	Residual	Coherence Factor
1	14	1.0633	350°	23	0.6687	354°	0.1624	0.8377
2	13	0.8902	349°	21	0.8383	353°	0.1627	0.8373
3	12	0.9499	348°	22	0.9542	353°	0.1909	0.8091
4	16	0.5372	350°	16	0.5372	350°	0.2871	0.7129

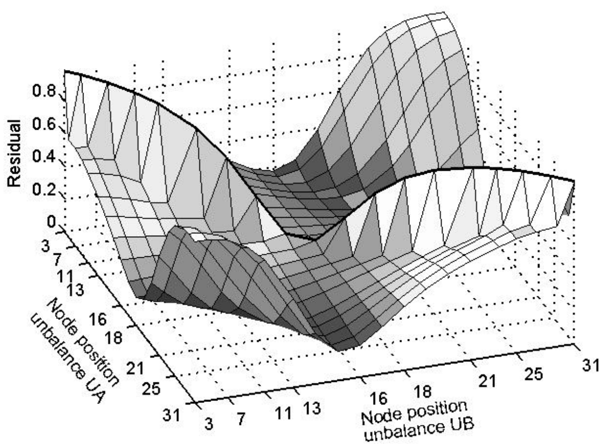

Figure 9. Map of the residuals associated with a pair of unbalances mounted on different cross-sections of the generator shaft.

The two unbalances associated with the lowest residual are reported in Table 3 (case 1) along with the results associated with some other pairs of unbalances that cause very small values of the residual. In fact, in this case study, more than one pair of unbalances is able to successfully simulate the generator experimental vibrations.

Single unbalance hypothesis

When the two unbalances are mounted on the same cross-section the nodes "A" and "B", as well as the unbalances UA and UB, coincide (case 4 of Table 3). In this case it is more difficult to find a single unbalance that is able to simulate the experimental dynamic behavior of the generator. Therefore, in the case of a single unbalance the residuals are rather high. Figure 10 shows the dependence of the residual on the axial position of two coincident unbalances: this curve coincides with that, illustrated in Figure 9, which connects the diagonal terms of the residual map. Very small residuals can still be obtained only when the only considered unbalance is applied to a short area close to the middle of the shaft. In fact, in this case, the generator normal mode associated with the critical speed n.7 (2538 rpm) is scarcely excited, in accordance with the experimental behavior, while the two normal modes associated with the critical speeds n.1 and n.2 (1041 rpm and 1372 rpm) are strongly excited, causing high vibration levels at bearings #1 and #2 in the speed range from 900 rpm and 1500 rpm.

However, in the middle of the generator rotor no maintenance activity was performed. Therefore, the analysis of the shape of the normal modes explains the reasons for which the fault identification method finds this interesting solution, however, in this case study, it must be discarded.

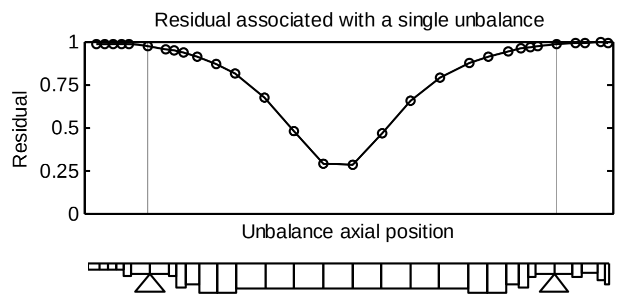

Figure 10. Dependence of the residual on the axial position of a single unbalance.

RELIABLE IDENTIFIED FAULTS

Very low values of the residual are obtained also by applying suitable pairs of unbalances in the area close to each cap of the generator: these unbalances must be nearly in phase.

Also in this case, owing to the shape of the normal modes associated with the three critical speeds of the generator contained in the range below 3000 rpm, very high vibrations can be generated in the rotational speed range from 900 rpm to 1500 rpm while only significantly lower vibration levels are caused in the speed range from 1800 rpm to 3000 rpm. In fact, when approaching the flexural critical speed of 2538 rpm, two unbalances of similar magnitude, mounted in phase to cross-sections close to the caps located at the opposite end of the main body of the generator rotor, cause a global work that is nearly null. That is the global energy introduced in the system by these two unbalances is rather small. This explains why the experimental dynamic behavior of the generator was affected by very high vibrations when passing through the first balance resonance and by minor vibration levels in the rotational speed range above 1800 rpm, in which the magnitude of the centrifugal forces caused by the residual unbalance significantly increases, without exciting the normal mode n.7, associated with the critical speed close to 2600 rpm that, before the maintenance, significantly affected the generator vibration in the speed range close to 3000 rpm.

In the following, a sensitivity analysis of the generator response to the effects caused by the identified unbalances, performed by means of a modal approach, is described.

Sensitivity analysis

The residual associated with a pair of unbalances located at nodes #13 and #21 ($\varepsilon = 0.1627$), that is at the cross-sections where the two caps are mounted, is very small and it is similar to the lowest residual ($\varepsilon = 0.1624$) obtained with the fault identification method for a pair of unbalances located at nodes #14 and #23.

Therefore, the unbalances located at nodes #13 and #21 have been considered the most likely cause of the abnormal dynamic behavior of the generator rotor found during machine runups and coastdowns. In fact, it is possible that maintenance activities performed in the area of the two caps and the final reassembling of the caps generated two unbalances. Considering the weight of the caps and the magnitude of the identified faults, the two unbalances are compatible with an eccentricity of the caps.

The Bode plot of the theoretical 1X transient vibration caused at bearing #1, in the X and Y directions, by the above mentioned unbalances is shown in Figures 11 and 12, respectively, along with the corresponding experimental data. The accordance between experimental vibrations and numerical results is rather good over the entire range of the rotational speed that has been considered.

The results reported in Table 3 show that the identified unbalances of the cases 1-3 are nearly in phase. Owing to the shape of the normal mode associated with the eigenvalue n.7 (Figure 8) this condition is essential to obtain that the global effect of the two unbalance forces weakly excites this normal mode causing only negligible vibration levels in the range of the rotational speed from 2300 rpm to 3000 rpm, in accordance with the experimental dynamic behavior. With regard to this, the 1X vibrations caused by the single unbalances applied at node #13 (case UA) and #21 (case UB) have been evaluated to emphasize the contribution of each excitation to the global response of the system. Figure 13 shows the Bode plot of these vibrations evaluated at bearing #1 in the X direction. In the same figure the amplitude and phase curves of the 1X vibrations caused by both unbalances (case UA and UB), along with the corresponding experimental data, are shown.

In the rotational speed range above 2000 rpm the amplitude of the vibration caused by each unbalance is considerable owing to the presence of the critical speed of the generator at 2538 rpm and to the significant increase of the magnitude of the centrifugal forces. However, in this speed range, the 1X vibrations caused by the unbalances UA and UB are out-of-phase and they have a similar amplitude: owing to this, their global effects are rather limited. Conversely, in the speed range from 900 rpm to 1500 rpm, in accordance with the shape of the normal modes n.1 and n.2 (Figure 8), the 1X vibrations caused by these two unbalances are nearly in phase: this causes very high vibration levels when passing through the first balance resonance of the shaft.

A further investigation has been carried out to point out the changes of the residual associated with different axial positions (node B) of the unbalance UB and a fixed location of the unbalance UA (node A).

Figure 14 shows the results obtained in three case studies in which the unbalance UA has been applied at the exciter (node #3) and at nodes #13 and #21.

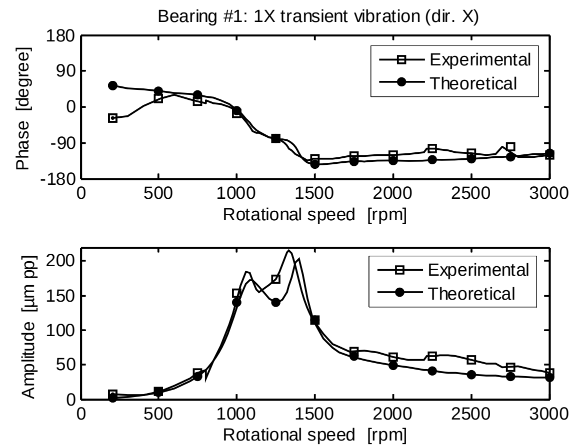

Figure 11. Bode plot of the 1X transient vibration at bearing #1 in the X direction: comparison between experimental data and numerical results (case 2).

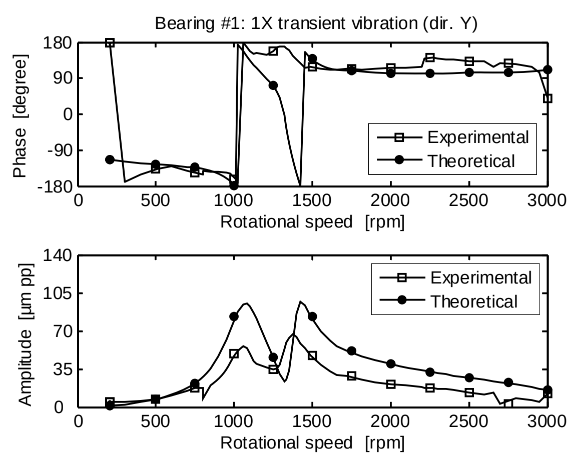

Figure 12. Bode plot of the 1X transient vibration at bearing #1 in the Y direction: comparison between experimental data and numerical results (case 2).

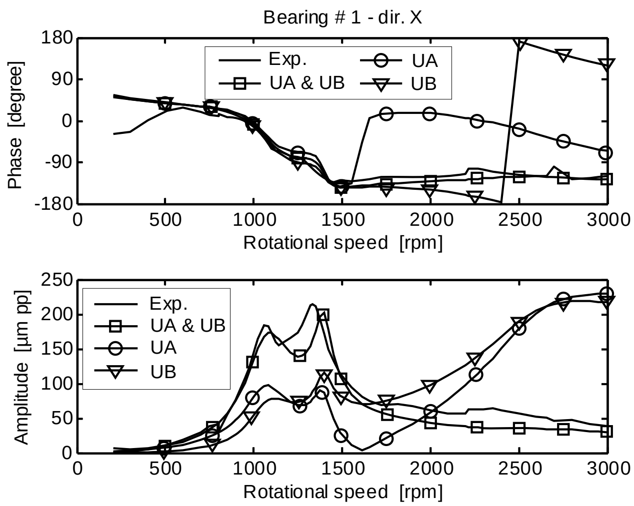

Figure 13. Transient vibrations, evaluated at bearing #1, in the X direction, caused by a single unbalance, UA, applied at node #13 or UB applied at node #21. UA and UB: vibration caused by both unbalances.

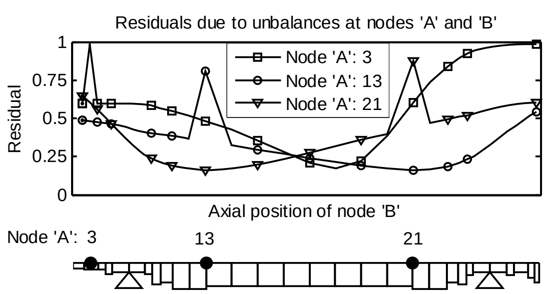

Figure 14. Residuals due to unbalances applied to different nodes "A" and "B".

It is possible to note that when the unbalance UA is mounted close to a cap of the generator rotor the lowest residual is obtained by applying the unbalance UB to the opposite end. Conversely, if the unbalance UA is mounted on the exciter, the lowest residual is obtained by applying the unbalance UB close to the middle of the shaft. Also these results are significantly influenced by the shape of the normal modes of the shaft contained in the range of interest of the rotational speed. Moreover, the dependence of magnitude and phase of the two unbalances on their axial position has been investigated.

Figure 15 shows the results obtained by fixing the position of the unbalance UA at node #13 and by changing the axial position of the unbalance UB along the generator rotor.

Depending on the position of the unbalance UB, the magnitude of the two unbalances is subjected to considerable changes. With regard to the relative angular position, the two unbalances can be in-phase or out-of-phase depending on their mutual position with respect to mid-span of the shaft.

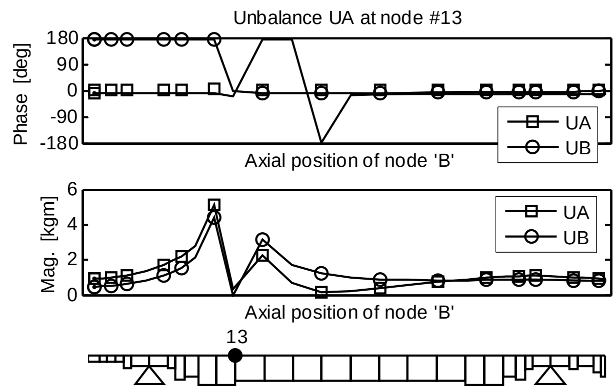

Figure 15. Dependence of magnitude and phase of unbalances UA and UB on the axial position of the unbalance UB (unbalance UA applied to node #13).

Modal approach

Rotating machine vibrations are significantly affected by the energy introduced by the excitations in the rotor system. A qualitative analysis of these phenomena can be performed by comparing the shape of the shaft-train normal modes to the axial position of the identified excitations that simulate likely faults. However, more useful quantitative results can be obtained by means of modal approaches that evaluate the sum of the Lagrangian components associated with each machine normal mode of interest. In fact, it is possible that in particular ranges of the rotational speed, also a set of excitations having a considerable magnitude introduces in the system only a negligible global energy.

In this case study, the contribution of the excitation of the normal modes n.1, n.2 and n.7 to the generator vibration has been investigated. With regard to this, it is important to consider that the frequency response of the system, $\bar{X}_j(\omega)$, evaluated at the *j*-th degree of freedom (d.o.f.) and at the exciting frequency ω, can be expressed as a function of the modal parameters as [7]:

$$\bar{X}_j(\omega) = \sum_{r=1}^{N} \frac{\sum_{k=1}^{M} \bar{\psi}_{jr}\,\bar{\psi}_{kr}\,\bar{F}_k(\omega)}{\left\{ m_r \left[\left(\omega_r^2 - \omega^2 \right) + \mathrm{i}\, 2\, h_r \omega_r \omega \right] \right\}} \tag{3}$$

where N is the number of normal modes contained in the frequency range of interest, M is the number of excitations applied to the system, ω_r is the *r*-th natural frequency, h_r (Table 2) and m_r are the modal damping factor and the modal mass associated with the *r*-th natural frequency. In the end, $\bar{\psi}_{jr}$ and $\bar{\psi}_{kr}$ are the complex components of the *r*-th normal mode evaluated at the *j*-th d.o.f., where the response is evaluated, and at the *k*-th d.o.f. to which the excitation $\bar{F}_k(\omega)$, due to an unbalance, is applied. The system eigenmodes have been normalized in order to obtain unitary modal masses m_r.

As we are interested in simulating the radial vibrations $\bar{X}_j$, caused by the identified unbalances, the *j*-th d.o.f. is that associated with the horizontal and vertical directions considered at the nodes of the shaft model that correspond to the generator journal bearings. On the basis of these results the radial vibrations in the X and Y directions, along which the sensors were mounted, have been evaluated.

The modal parameters of the rotor system have been obtained by evaluating the eigenvalues and eigenmodes of the model of the fully assembled machine. The contributions of the normal modes from n.3 to n.6 to the generator response have been considered negligible as they mainly affect the dynamic behavior of the steam turbines of the power unit.

Figure 16 shows a comparison between the experimental vibrations measured at bearing #1, in the X direction, and the respective global response obtained by substituting the modal parameters into the eq.(3) in which the centrifugal forces associated with the two identified unbalances applied at nodes #13 and #21 have been considered as excitations. The accordance between experimental data and numerical results is very good.

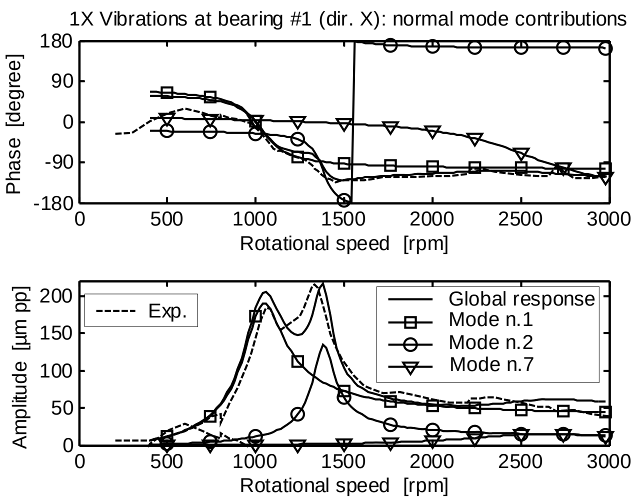

Figure 16. Contribution of the modes n.1, n.2 and n.7 to the vibrations evaluated at bearing #1, in the X direction. Comparison between experimental data and the response evaluated by means of the modal parameters of the rotor system.

Moreover, the contribution of each normal mode to the generator response evaluated by means of the modal parameters has been investigated. To this purpose, the eq.(3) has been used considering only one normal mode at a time. The 1X transient vibrations caused at bearing #1, in the X direction, by the excitation of the single normal modes n.1, n.2 and n.7 (Table 2, Figure 8) are shown in Figure 16.

It is possible to note that, also in the rotational speed range above 2000 rpm, the amplitude of the vibration caused by the excitation of the first normal mode is not negligible: on the contrary, it gives the main contribution to the level of the vibrations measured at the operating speed.

With regard to this, it is necessary to consider that the excitations $\bar{F}_k(\omega)$ that are contained in the numerator of eq.(3) are caused by the identified unbalances: therefore, their magnitude significantly increases with the rotational speed. In the speed range above 1500 rpm this effect compensates the noticeable decrease of the term associated with the first natural frequency, contained in the denominator of eq.(3). Moreover, the results illustrated in Figure 16 confirm that owing to the axial position and the phase of the identified unbalances, as well as to the shape of the normal mode n.7, the resonance of the generator close to 2600 rpm is weakly excited.

CONCLUSION

A model-based diagnostic strategy has been used in the paper to identify the faults that cause abnormal vibrations in a rotating machine. However, the identified faults that are able to satisfactorily simulate the experimental dynamic behavior of the shaft-train can be more than one.

The analysis of the dynamic behavior of a large power unit has shown that significant diagnostic information can be obtained by taking into account the modal parameters of the rotor system and their effects on the machine frequency response. These information can be very useful to understand which is the most likely fault among those found by the fault identification method. This differentiates this method from those of other authors.

REFERENCES

1. Lalanne M., Ferraris G., *Rotordynamics Predictions in Engineering*, (1998), John Wiley & Sons Inc., Chichester, England.
2. Adams M., *Rotating machinery vibration*, (2001), Marcel Dekker Inc., New York, N.Y., USA.
3. Markert R., Platz R., Seidler M., *Model Based Fault Identification in Rotor Systems by Least Squares Fitting*, Proc. ISROMAC-8 Int. Symposium on Transport Phenomena and Dynamics of Rotating Machinery, Texas A&M University, 2, (2000), pp. 901-907.
4. Bachschmid N., Pennacchi P., Vania A., *Identification of multiple faults in rotor systems*, Journal of Sound and Vibration, 254, No.2, (2002), pp.327-366.
5. Isermann R., *Supervision, fault-detection and fault diagnosis methods: an introduction*, Control Engineering Practice 5 (5), (1997), pp.639-652.
6. Lees A.W., Friswell M.I., *The evaluation of rotor imbalance in flexibly mounted machines*, Journal of Sound and Vibration, 208, (5), (1997), pp.671-683.
7. Ewins D. J., *Modal Testing: Theory and Practice*, (1984), John Wiley and Sons, London.

